

Proceedings of the JMSM 2008 conference

## Elaboration and characterization of thin solid films containing cerium

S. Hamdi<sup>a</sup>, S. Guerfi<sup>b</sup>, R. Siab<sup>a\*</sup>

<sup>a</sup>Centre Universitaire El Tarf, 36000, Algeria

<sup>b</sup>Badji Mokhtar University Annaba, 23000, Algeria

Received 1 January 2009; received in revised form 31 July 2009; accepted 31 August 2009

---

### Abstract

Cerium oxide films are widely studied as a promising alternative to Cr(VI) based pre-treatments for the corrosion protection of different metals and alloys. Cathodic electrodeposition of Cerium containing thin films was realised on TA6V substrates from a  $\text{Ce}(\text{NO}_3)_3$ ,  $6\text{H}_2\text{O}$  and mixed water-ethyl alcohol solutions at 0.01 M. Experimental conditions to obtain homogeneous and crack free thin films were determined. The deposited cerium quantity appears proportional to the quantity of electricity used, as indicated by the Faraday law. Subsequent thermal treatment lead to a  $\text{CeO}_2$  coating, expected to provide an increase of TA6V oxidation resistance at high temperatures. The deposits were characterized by differential scanning calorimetry (DSC), optical and scanning electron microscopies.

© 2009 Elsevier B.V. All rights reserved

PACS: Type pacs here, separated by semicolons ;

Keywords: Electrolytic deposition; Cerium oxide; Cathodic deposit; Titanium alloy.

---

### 1. Introduction

Titanium and its alloys have been considered as one of the best engineering materials for use in industrial application due to their high specific strength, good corrosion resistance and biocompatibility [1-3]. However, a major problem of titanium alloys is an insufficient wear resistance and serious oxidation at high temperature [4,5]. To combat this problem, conversion coatings are widely used as part of the corrosion protection system [6].

The use of rare-earth compounds particularly cerium compounds have attracted significant attention for corrosion protection of metals and alloys as a result of new environmental regulations to replace toxic compounds [7, 8].

Cathodic electrodeposition has been used because of the low cost of equipment and of precise control of deposited thickness [9,10].

The focus of this study is on cerium based conversion coatings, which have shown promise as potential replacements for chromates [11,12]

---

\* Corresponding author. Tel.: +213-78-714-721; fax: +213-38-601-533.  
E-mail address: [rachsiab@yahoo.fr](mailto:rachsiab@yahoo.fr).

In the present work, an electrodeposition technique was used to get, in one step, thin cerium containing films over all surfaces of TA6V samples. The deposits were then submitted to a thermal treatment under argon in order to get a  $\text{CeO}_2$  coating, the aim being to later study the behaviour of such a coated material under high temperature oxidation conditions.

## 2. Experimental procedures

In all experiments, coupons were cut from a commercial TA6V alloy rod (Ti-6wt.% Al-4wt.%V), with 10mm in diameter and approximately 2mm in thickness, and drilled to get a 1,5mm hole for suspension. Samples were abraded from 600 SiC paper to  $3\mu\text{m}$  diamond paste, ultrasonically cleaned in acetone, water and ethanol and then dried with pulsed warm air before use. A chemical attack by Kroll's reactant (2vol.% hydrofluoric acid and 3vol.% nitric acid in water) showed that TA6V alloy presents a two-phase structure (95.4% hexagonal  $\alpha$ -phase and 4.6% cubic  $\beta$ -phase) (see Fig. 1), explaining that this is one of the most employed titanium alloys, being a compromise between  $\alpha$ -alloys, having the best weldability, and  $\alpha+\beta$  alloys, being the most mechanically resistant.

### 2.1. Experimental set-up for cathodic electrodeposition

The electrochemical bath was a 0.01 M  $\text{Ce}(\text{NO}_3)_3$  solution, obtained by dissolving commercial cerium nitrate ( $\text{Ce}(\text{NO}_3)_3 \cdot 6\text{H}_2\text{O}$ , 99.99% purity) in water 50 vol.% ethyl alcohol. Electrodeposition was realised using a classical three electrode experimental set-up, described elsewhere [13,14], including a TA6V sample as cathode, a platinum grid counter electrode and a saturated calomel electrode (SCE) as reference.

Deposition experiments were carried out in galvanostatic mode, current density varying from  $j = -2$  to  $-0.05 \text{ mA cm}^{-2}$ , at ambient temperature and without stirring. Deposition time was varied from 100 to 7200 s. The variation of the potential versus time was recorded during deposition. After electrodeposition, samples were rinsed with ethyl alcohol and air dried for at least a night before further use or analysis.

These experimental conditions were chosen from previous work [14] and were expected to provide thin films with a thickness in the range 50–500 nm.

### 2.2. Deposited and thermally treated films characterization

Different analytical techniques have been used to characterize the deposited film and its behaviour during conversion thermal treatment. Deposit morphology was observed by optical and scanning electron microscopies (OM, SEM). A deposit formed at  $j = -0.2 \text{ mA cm}^{-2}$  during 7200 s was scratched off from the substrate surface, such a scratched off deposit was also used for differential scanning calorimetry (DSC 2010/2920 cell, TA instruments-universal analysis 2000): it was placed in an aluminium nacelle and heated from 40 to  $560 \text{ }^\circ\text{C}$  at  $10 \text{ }^\circ\text{C min}^{-1}$ , then cooled down to room temperature and finally submitted to a second thermal cycle.

The quantity of deposited cerium versus deposition time has been determined using inductively coupled plasma-optical emission spectroscopy (ICP-OES). Deposits formed at  $j = -0.2 \text{ mA cm}^{-2}$  for 100–7200 s duration were dissolved in a water 5 vol.% nitric acid solution and the obtained solutions were analysed following the usual procedure for this technique.

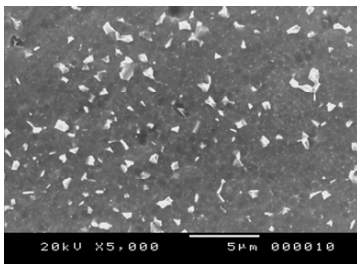


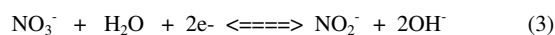
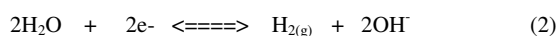
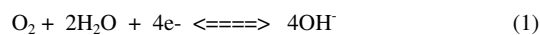
Fig. 1. SEM micrograph showed that TA6V alloy presents a two-phase structure (95.4% hexagonal  $\alpha$ -phase and 4.6% cubic  $\beta$ -phase).

### 3. Results and discussion

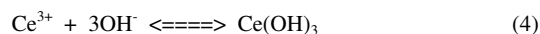
#### 3.1. Electrodeposition

Electrochemical mechanism during cathodic deposition has been widely discussed in the literature [15–18]. Two steps have to be distinguished [19-21].

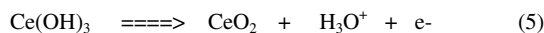
The first one corresponds to the cathodic generation of hydroxyl ions, OH<sup>-</sup>, by reduction of O<sub>2</sub>, H<sub>2</sub>O or NO<sub>3</sub><sup>-</sup>, etc.



The second should be the precipitation reaction of Cerium hydroxide. The formation of hydroxyl ions at the cathode leads to local increase of the pH at the surface that promotes the formation of a Ce(OH)<sub>3</sub> precipitate (Eqs.(4)).[18].



The Cerium oxide film then results from the oxidation of Ce(OH)<sub>3</sub> (Eq. (5)) [15,18].



The electrochemical mechanism of formation of these oxide films is really complex. Li and Thompson [18] suggested that the deposition of the solid film proceeded through a nucleation and growth process.

#### 3.2. Polarization experiments

Cathodic polarization curves for TA6V in a mixed water–ethanol solution of cerium nitrate, without stirring, are shown in Fig. 2. Addition of ethyl alcohol reduces the total dielectric constant of solvent and decreases the double layer thickness promoting particle coagulation and gel formation [13]. The polarization curves obtained with unstirred solution can be divided in different potential domains. For the first domain, at potentials higher than -0.1.1 V/SCE, the low current densities observed correspond to reduction of dissolved oxygen (Eq. (1)).

In the second domain (from -1.1 to -1.6 V/SCE), the cathodic current density quickly increases, reaction taking place being the reduction of water to form H<sub>2</sub> (Eq. (2)). From -1.6 to -1.8 V/SCE, current density reaches a steady state value ( $j = 0.8 \text{ mA cm}^{-2}$ ). This phenomenon is attributed to the surface blocking by the film formed by precipitation with hydroxyl ions previously produced. Further continuation of potential scan towards cathodic potential results in an increase of current density due to hydrogen evolution reaction (Eq. (2)). At the same time, strings of H<sub>2</sub> gas bubbles start being observed. This feature may indicate that the film previously formed on the metal undergoes local breakdown manifested in gas bubbles, creating sites of stronger reduction current.

#### 3.3. Galvanostatic deposition

Experiments performed on galvanostatic mode, without stirring, varying cathodic current density, revealed deposit formation even for very low current densities, showing that the local rise in pH responsible for the

precipitation is effective. The effect of current density on film morphology has been investigated in order to obtain homogeneous and crack free thin films. For a current density of  $-1 \text{ mA.cm}^{-2}$ , the film formation is rapid and very important cracks can be observed at the scanning electron microscopy (see Fig. 3).

To avoid the occurrence of cracking, smaller intensity values, ranging from  $-0.05$  to  $-0.2 \text{ mA.cm}^{-2}$  were then retained in order to lower the electrodeposition rate. Fig. 4 gives the variation of potential versus time during deposition, at  $j = -0.05, -0.1$  and  $-0.2 \text{ mA.cm}^{-2}$ . In every case, a very quick decrease of potential is observed in the first few seconds, corresponding to current stabilisation, then a transition period and, finally, a regular decrease of potential as film thickens.

An homogeneous film (Fig. 5) is obtained after a 1800 s deposition time under  $j = -0.2 \text{ mA.cm}^{-2}$  and this current density has been chosen for further characterisation.

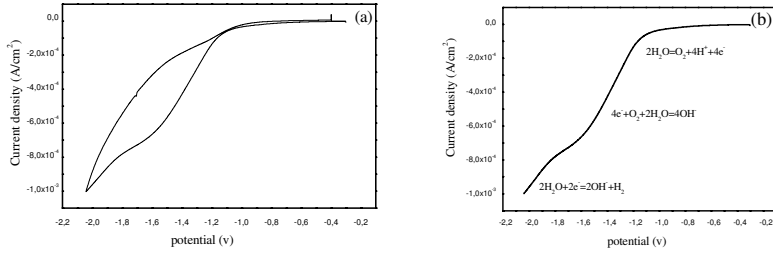


Fig. 2. Cyclic voltammety curves obtained with TA6V substrates in  $\text{Ce}(\text{NO}_3)_3$ ,  $6\text{H}_2\text{O}$  and mixed water-ethyl alcohol solutions at  $0.01 \text{ mol.L}^{-1}$ , ( $10 \text{ mV/s}$ ).

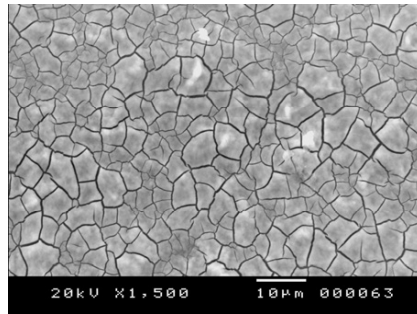


Fig. 3. SEM micrograph of cerium containing deposit ( $j = -1 \text{ mA.cm}^{-2}$ , deposition time 1800s), showing the cracking of the film

### 3.4. Electrodeposited cerium quantity

The quantity of deposited cerium versus deposition time, at  $j = -0.2 \text{ mA.cm}^{-2}$  current density, dissolved in  $\text{HNO}_3$ , has been determined using ICP-OES. A linear variation of cerium quantity with time can be observed on Fig. 6. The deposited cerium quantity appears proportional to the quantity of electricity used, as indicated by the Faraday law. This variation provides an easy control of the film thickness, for the fixed conditions. Moreover, these results are close to those obtained by I. Zhitomirsky and al. on Pt substrates [13] and suggest that mechanism and deposition rate are independent of metallic substrate nature.

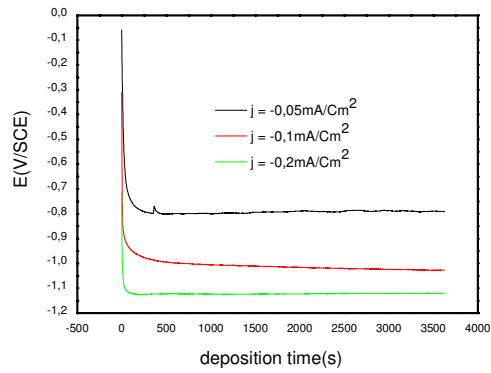


Fig. 4. Variation of potential vs. time during cathodic deposition at  $j = -0.05, -0.1$  and  $-0.2 \text{ mA cm}^{-2}$

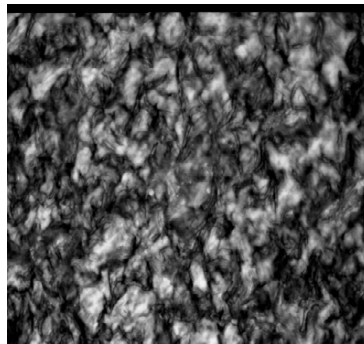


Fig.5. Optical micrograph of cerium containing deposit ( $j = -0.2 \text{ mA.cm}^{-2}$ ).

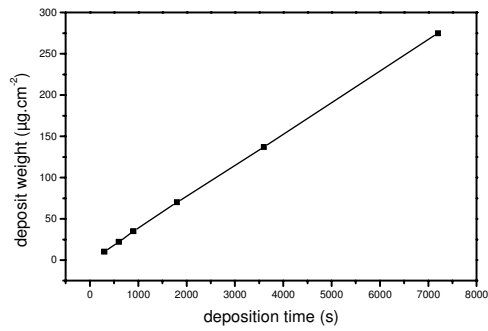


Fig.6. ICP-OES measurements of the deposited cerium amounts vs. time (current density  $j = -0.2 \text{ mA.cm}^{-2}$ )

### 3.5 Effect of heat treatment

Heat treatment was applied on deposited films in order to promote dehydration [22], interdiffusion and adhesion [23] of deposit on metallic substrate. Results of thermal analysis (DSC) of  $\text{Ce}(\text{OH})_3$  powder are presented in Fig. 7. It can be observed that two exothermic peaks at 200 and 450 °C appear during the first heating. Cooling curve and second heating curve demonstrated that all the transformations are irreversible. These results are close to those obtained by I. Zhitomirsky and al, studied by differential thermal analysis (DTA) [24]. In fact this author observed two successive weight changes at different temperatures. The first one, below 200 °C, seemed to originate from the water loss associated with  $\text{Ce}(\text{OH})_3$ . The second one, approximately 450 °C, was related to the conversion of hydroxide into oxide. This sequence appears satisfactory to interpret the two exothermic peaks observed in our analysis.

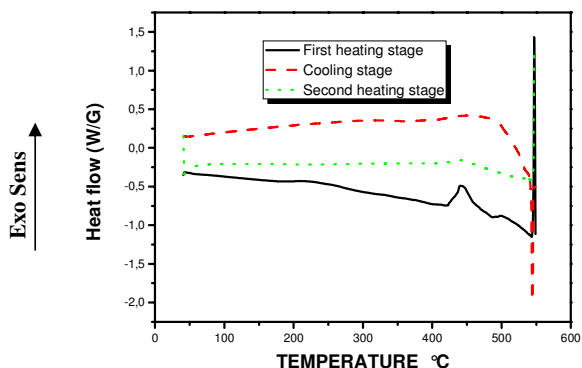


Fig.7.DSC analysis of scratched off deposit from 40 to 560 °C at 10 °C.min<sup>-1</sup>.

### Conclusions

The aim of this work was to determine adequate parameters for cathodic electrolytic deposition, on TA6V substrate, of cerium hydroxide films from mixed water–ethyl alcohol solutions to obtain, after a thermal treatment, thin  $\text{CeO}_2$  films (<500 nm), suitable for high temperature purposes. The deposit weight and hence the deposit thickness was shown to increase with current density at a constant deposition time. However, low current densities ( $-0.2 \text{ mA.cm}^{-2}$ ) promoted the formation of thin, crack-free films (which was not the case for higher current densities). The deposited cerium quantity appears proportional to the quantity of electricity used, as indicated by the Faraday law. Microscopic observations ( $-0.2 \text{ mA.cm}^{-2}$ ) revealed that formed cerium hydroxide films are uniformly deposited all over the sample surfaces. The results of the DSC analysis are in perfect concordance with the literature. This study thus illustrates that electrolytic deposition can be used to obtain thin and uniform cerium films over a metallic substrate used as the cathode. High temperature oxidation experiments are currently performed on coated specimens. First results are quite promising.

### Acknowledgements

The authors are greatly thankful to M. Bordes (CCA la Rochelle University) for her contribution to Scanning Electron Microscopy analysis and to S. Cohendoz (Lemma la Rochelle University) for his valuable help on DSC analysis.

## References

- [1] N.Kahraman, B.Gulenc, F.Findik, *Int.J. Impact Eng.* 34 (2007) 1423.
- [2] J.E.G. Gonzalez, J.C.Mirza-Rosca, *J. Electroanal. Chem.* 471 (1999) 109
- [3] W. Kathy, *Mater.Sci. Eng.* 213A (1996) 134
- [4] Z. Zufang, Chemical Industry Press, Beijing, 1999, p.75
- [5] R.W. Schutz, Japan International. SAMPE Symposium, 1993, p.7
- [6] D. Baudrond, *Plating and Surface Finishing* 92(1) (2005) 30-35
- [7] M. Bethencourt, F.J.Botana, M.J. Cano, M.Marcos, *Applied Surface Science* 238 (2004) 278
- [8] A. Decroly, J.P. Petitjean, *Surface & Coatings Technology* 194 (2005) 1
- [9] Y. Zhou, J.A. Switzer, *J.Alloys Compd.* 237 (1996) 1
- [10] P. Stefanov, G.Atanasova, D. Stoychev, T.S. Marinova, *Surf.Coat. Technol.* 180-181 (2004) 446.
- [11] F.W. Lytle, R.B. Greigor, G.L. Bibbins, K.Y. Blohowiak, R.E. Smith, G.D. Tuss, *Corr. Sci.* 37(3) (1995) 349-369
- [12] W.G. Fahrenholtz, M.J. O'Keefe, H. Zhou, J.T. Grant, *Surf. Coat. Technol.* 155 (2002) 208-213
- [13] I. Zhitomirsky, A. Petric, *Mater. Lett.* 50 (2001) 189
- [14] J.M. Brossard, G.Bonnet, J.Balmain, J.Creus, *Surf. Coat. Technol.* 185 (2004) 275
- [15] M. Balasubramaniam, C.A. Melendres, A.N. Mansour, *Thin Solid Films* 347 (1999) 178
- [16] A. Qi Wang, T.D. Golden, *J. Electrochem. Soc.* 150 (2003) C616
- [17] T.D. Golden, A. Qi Wang, *J. Electrochem. Soc.* 150 (2003) C621
- [18] E.B. Li, G.E. Thompson, *J. Electrochem. Soc.* 146 (1999) 1809
- [19] I.Zhitomirsky, *Adv. Colloid Interf.Sci.* 97 (2002) 279
- [20] L. Gal-Or, I. Silberman, R. Chaim, *J.electrochem .Soc* 138 (1991) 1939
- [21] S. Peulon, D. Lincot, *J. Electrochem. Soc.* 145 (1998) 864
- [22] J. Creus, F. Brezault, C. Rebere, M. Gadouleau, *Surf. Coat. Technol.* 200 (2006) 4636-4645
- [23] I. Zhitomirsky, A. Petric, *J. Mater. Chem.* 10 (2000) 1215
- [24] I. Zhitomirsky, A. Petric, *J. Materials Letters* 40 (1999) 263–268